

UNCLASSIFIED

Defense Technical Information Center
Compilation Part Notice

ADP011107

TITLE: Analysis of Jet Interaction for Supersonic Flow Control

DISTRIBUTION: Approved for public release, distribution unlimited

This paper is part of the following report:

TITLE: Active Control Technology for Enhanced Performance Operational Capabilities of Military Aircraft, Land Vehicles and Sea Vehicles
[Technologies des systemes a commandes actives pour l'amelioration des performances operationnelles des aeronefs militaires, des vehicules terrestres et des véhicules maritimes]

To order the complete compilation report, use: ADA395700

The component part is provided here to allow users access to individually authored sections of proceedings, annals, symposia, etc. However, the component should be considered within the context of the overall compilation report and not as a stand-alone technical report.

The following component part numbers comprise the compilation report:

ADP011101 thru ADP011178

UNCLASSIFIED

Analysis of jet interaction for supersonic flow control

E. Collin, S. Barre and J.P. Bonnet

LEA/CEAT, Université de Poitiers

43, route de l'Aérodrome, 86036 POITIERS CEDEX (France)

Phone : 33 5 49 53 70 15

Fax : 33 5 49 53 70 01

E-Mail : erwan.collin@lea.univ-poitiers.fr

1. Introduction

In a lot of industrial applications, especially in ejectors and propulsive jets, most of the dynamical behaviour of the system is strongly influenced by the mixing efficiency in a supersonic jet. This is particularly the case when dilution of hot propulsive jets is required for example to reduce infrared signature of a military aircraft. Many mechanical devices have been used to increase mixing in free shear flows. Most of these devices stimulate the activity of longitudinal vortices naturally occurring in mixing layers¹. For instance, the insertion of small tabs on the splitter plate of a plane mixing layer, or in the nozzle of a jet, produces large and small-scale vortical motions². This results in a strong distortion of the mean flow and a strong mixing enhancement^{3,4,5}.

In order to prepare the development of an active hyper-mixing method, Davis⁶ studied a pneumatic device. A schematic arrangement of this device is shown in figure 1. It is generally admitted that transverse jets generate longitudinal vorticity in a crossflow. Several control jets (CJ) can be used in order to improve the mixing in the initial part of a supersonic jet. This kind of device has been proved to be efficient in subsonic flows⁶. The question arises of the behaviour of such control jets in supersonic flows.

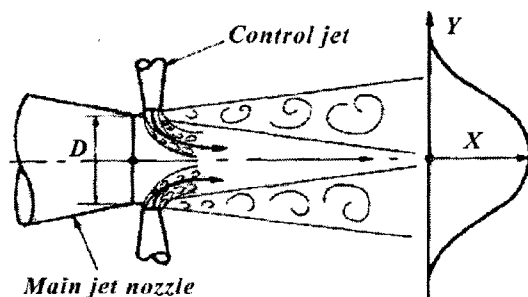


figure 1

General arrangement of the pneumatic device
(from Davis⁶)

A parametric study has been done by Collin et al⁷ in order to evaluate the effects of one CJ dynamic pressure and geometry on the mixing enhancement in the case of a $M=1.37$ cold jet. Pressure and temperature measurements in the far field region of the interaction between the CJ and the main jet revealed a strong distortion of the mixing layer. This distortion is shown on figure 2 and looks like the one obtained with tabs. The manipulated mixing layer

has shown to be locally twice thicker under the action of the CJ (see figure 3). However, as shown on figure 4, no augmentation of the spreading rate has been noticed in the far field (e.g. one diameter or more downstream the main jet nozzle). Although the effects of the dynamic pressure ratio between the CJ and the main jet were almost understood, the effects of the CJ nozzle geometry were not clear at all. For all these reasons, we intended to realise some visualisations in the near field of the interaction between a main supersonic jet and only one control jet.

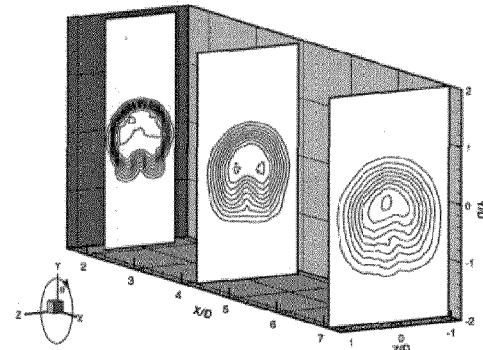


figure 2
Longitudinal evolution of the velocity distribution in cross-sections of the manipulated supersonic jet
(from Collin et al⁷)

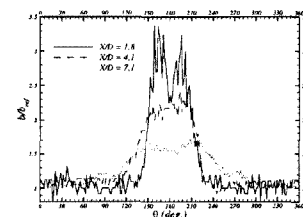


figure 3
Azimuthal distribution of the mixing layer thickness
(from Collin et al⁷)

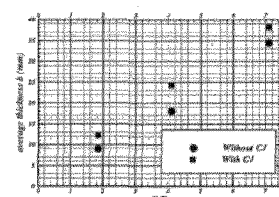


figure 4
Longitudinal evolution of the averaged mixing layer thickness (from Collin et al⁷)

The visualisations obtained for fixed dynamic pressure ratio and CJ nozzle geometry are described in §3. These visualisations show a local augmentation of the spreading rate of the mixing layer. Whereas a strong intermittent behaviour is detected for the penetration of the CJ in the mixing layer, longitudinal vorticity has been put forward just downstream the CJ. In the §4, we present some visualisations obtained for 3 different CJ nozzles, in order to explain the effects of the CJ geometry.

2. Experimental set-up

2.1. Wind tunnel

The wind tunnel used in this study is the *S150* high-pressure facility of the *C.E.A.T.* of Poitiers, France. This is a $M=1,37$ supersonic jet surrounded by a subsonic entrained coflow. Stagnation pressure and temperature for the main jet are respectively 3bar and 260K . The coflow velocity and stagnation temperature are 47ms^{-1} and 290K . The convective Mach number is $M_c=0.49$. The supersonic jet has the same static pressure than the subsonic coflow. The nozzle diameter is $D=50\text{mm}$. The test section is $500 \times 500 \text{ mm}^2$. A 200bar dry air tank supplies the main jet.

2.2. Actuators

The CJ is supplied by the same 200bar dry air tank as the main jet and is placed 5mm downstream and 5mm bellow the main jet nozzle. The CJ stagnation pressure is kept constant at 2.5bar. The picture of figure 5 shows the test section, with the main jet and the CJ. Three different CJ nozzles (two rectangular and one circular) are used in order to understand the effects of the CJ geometry. Their description is given in table 1.

Type	Shape	Φ_{ea}	$L \times d$	L/l	position
Rect1	Rectangular	3.7	11×1	11	► □
Rect2	Rectangular	5	9.5×2	4.75	► □
Circ	Circular	5			► ○

table 1

Descriptions of the control jet nozzles used in the study
(dimensions are given in mm)

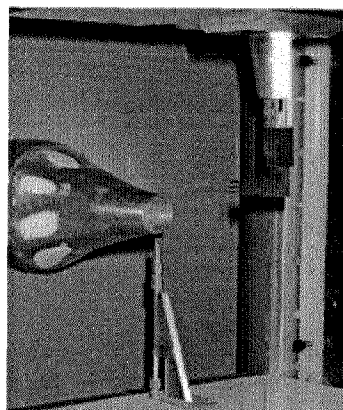


figure 5
Photography of the *S150* test section

2.3. Visualisation technique

Visualisations of the flow are obtained with a PIV system. A laser sheet is realised with a Nd YAG pulsed laser beam. Pictures are acquired on computer by the use of a CCD camera. The time of exposure is about 6ns, which is short enough to 'freeze' the flow.

Several kinds of visualisations are realised with different laser sheet and camera positions. Side views are easily performed thanks to large windows in the walls of the test section. The realisation of end views pictures (i.e. cross sections of the flow) is much more challenging. When we intend to have a global point of view of the cross sections, we install the camera in the diffuser. For more zoomed images, we have to realise 'pseudo-end' views from the side of the test section. That is to say that the camera is not strictly recording cross sections. Although, the angle between the laser sheet and the cross section of the tunnel never exceeds 14° .

Three seeding techniques are used: natural seeding, ethanol droplets and SiO_2 particles. Natural seeding is obtained by condensation of the surrounding air mixed with the cold supersonic jet. This technique is used for cross-sectional views of the mixing layer itself in the far field region of the interaction. Ethanol droplets and SiO_2 particles are used in the very near field of the interaction. Side views of the mixing layer in this region are realised by seeding the boundary layer inside the main jet nozzle with ethanol droplets. Side and cross-sectional views of the CJ are done with a CJ seeded with SiO_2 particles.

2.4. Data analysis

We acquire 200 instantaneous pictures at 10Hz . Each picture has 768×484 pixels, coded on 256 greyscale levels. Very simple homemade algorithms give well-converged average and *rms* picture for each run.

3. Results for one CJ geometry

This part of the study concerns the understanding of the mechanisms involved in the interaction between one CJ and the main jet. The CJ used here is type *rect1*, with a stagnation pressure of 2.5bar.

3.1. Structures of the CJ

3.1.1. Cross-sectional views

The longitudinal aspect of the structures of the CJ is obtained with a laser sheet almost perpendicular to the main undisturbed jet. The CJ is seeded with SiO_2 particles. The figure 6 and figure 7 show respectively the average and the *rms* pictures obtained for three downstream positions. We can easily notice that the CJ is flattened when it reaches the mixing layer. Far downstream, the CJ is deformed.

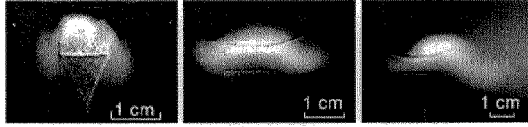


figure 6

Cross-sectional average views of the structures of the CJ (from left to right: $X/D=0.14, 0.4$ and 1.0)

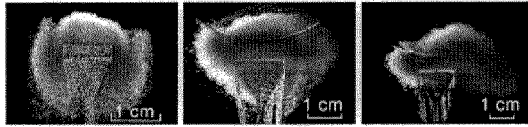


figure 7

Cross-sectional rms views of the structures of the CJ (from left to right: $X/D=0.14, 0.4$ and 1.0)

The figure 8 shows instantaneous pictures obtained in the cross-sections. These visualisations put forward the formation of small-scale longitudinal vorticity in the very first stage of the CJ. The small longitudinal vortices seem to reconnect themselves downstream. At the last cross-section, we can easily identify a pair of counter rotating vortices. However, it seems that an intermittent behaviour destabilise the longitudinal vortices. This behaviour is analysed thanks to side views visualisations.



figure 8

Cross-sectional instantaneous views of the CJ (from left to right: $X/D=0.14, 0.4$ and 1.0)

3.1.2. Side views

Here, the laser sheet is positioned in the median plan of the main jet. The CJ is seeded with SiO_2 . The figure 9 shows average and *rms* pictures. The main flow is from left to right. The trajectory of the CJ looks like the one obtained with jets in cross flows. However, the curvature seems to be much more important in the region where the CJ is impinging the main supersonic jet, and the CJ spreads downward. The average picture shows also that the CJ turns into the mixing layer.

The *rms* side view indicates that the boundaries of the CJ are turbulent. We can also notice that a part of the CJ turns upstream, very near the CJ nozzle. This behaviour is better understood in the analysis of the instantaneous pictures.

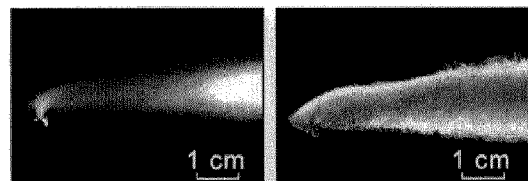


figure 9

Average (left) and rms (right) side views of the CJ

Close-up instantaneous views are represented in figure 10. We can see that we have two kinds of behaviour: either the CJ penetrates deeply in the mixing layer, or it is completely stopped when it reaches the mixing layer.

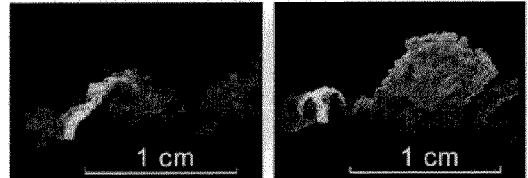


figure 10

Instantaneous side views of the structures of the CJ

Two kinds of phenomenon can explain this behaviour. First, as the CJ size is quite small, it is possible that the penetration depends on the presence of a Kelvin-Helmoltz structure in front of the CJ exit. Indeed, if the adverse pressure gradient were sufficiently strong just upstream a Kelvin-Helmoltz rollup, the penetration of the CJ would decay. On the other hand, when the CJ nozzle is facing the rear of a Kelvin-Helmoltz roll up, the penetration is furthered. However, this hypothesis implies that the Kelvin-Helmoltz rollups generate very strong pressure fluctuations.

The other hypothesis we can make in order to explain this intermittent behaviour is based on an intrinsic instability of the interaction between the CJ and the annular mixing layer. This instability may be due to the generation of a high-pressure region just upstream the CJ, caused by a local downward deviation of the main jet. When the pressure upstream the CJ is sufficiently strong (i.e. at least equal to the CJ stagnation pressure), the high-pressure zone is convected downstream, stopping the penetration of the CJ. Unfortunately, we would need further measurements and simulations in this way to confirm if the intermittent penetration behaviour is due to this kind of mechanism.

3.2. Structures of the manipulated mixing layer

3.2.1. Cross-sectional views

Cross-sectional views of the manipulated jet are realised from the wind tunnel diffuser. The seeding is obtained by condensation of the surrounding air when mixed with the cold main supersonic jet. The figure 11 shows three instantaneous pictures taken at $X/D=3, 4.1$ and 7.1 . These pictures look like the mean flow measurements obtained previously (see figure 2). The visual aspect of these structures seems to be almost steady.

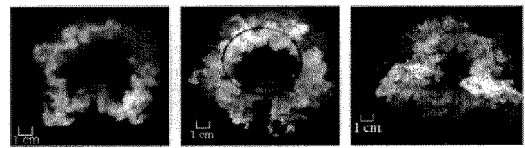


figure 11

Instantaneous cross-sectional views of the manipulated mixing layer (from left to right: $X/D=3, 4.1$ and 7.1)

3.2.2. Side views

Here, the seeding is realised by the addition of ethanol droplets inside the boundary layer in the settling chamber of the main supersonic jet.

The figure 12 shows the average and *rms* pictures obtained with a 200 pictures data set. The average picture puts forward the mixing enhancement very near the CJ exit. The spreading rate can be evaluated with the visual thickness. A comparison between the upper (unperturbed) and the lower (manipulated) mixing layer of the figure 12 leads to :

$$\frac{\Delta\delta_{viz}}{\Delta x} \Big|_{with\ CJ} \approx 1,2 \cdot \frac{\Delta\delta_{viz}}{\Delta x} \Big|_{without\ CJ}$$

The action of the CJ leads to a spreading rate 20% bigger very near the injection. The mixing layer thickness is increased just in front of the CJ.

The *rms* picture reveals a very intermittent phenomenon occurring just upstream the CJ.

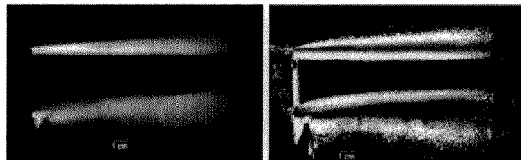


figure 12
average and rms side views
of the manipulated mixing layer

Two examples of instantaneous side views are given in figure 13. These pictures may indicate a strong acceleration of the Kelvin-Helmoltz rollups. Indeed, structures looking like Kelvin-Helmoltz's are more distinct under the action of the CJ. An approximation of the Strouhal number can be done with the definition:

$$St = \frac{F \cdot \delta_\omega}{U_c} \approx \frac{\delta_\omega}{l}$$

where l is the longitudinal structure spacing.

Taking the height of the structures for δ_ω , we obtain $St \approx 0.55$. As a comparison, the Strouhal number of the unperturbed mixing layer is approximately 0.3. However, this must not mean that the CJ develops the second or the third sur-harmonic of the mixing layer instability: this just means that the aspect ratio of the structures of the mixing layer is completely changed under the action of the CJ. Indeed, by keeping constant the convective velocity and the Kelvin-Helmoltz instability frequency, we just have to increase the thickness to change the Strouhal number.

On the right hand of figure 13 we can see a different behaviour of the CJ penetration. A part of the flow issuing from the main jet nozzle turns down just upstream the CJ. This may be caused by the unsteady penetration of the CJ (see §3.1.2). The fact that a part of the mixing layer is turned down upstream the CJ may imply that the

unsteady behaviour of the CJ penetration is due to an intrinsic instability of the interaction between a transverse jet and a free shear flow.

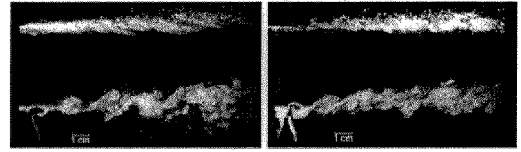


figure 13
Two examples of instantaneous side views
of the manipulated mixing layer

Finally, several remarks can be deduced from the visualisations obtained with a single CJ. First, side views of the manipulated mixing layer show an enhancement of the spreading rate near the injection. Secondly, instantaneous cross-sectional pictures revealed the presence of a pair of counter-rotating vortices generated by the CJ. However, these vortices are not steady at all. A very intermittent behaviour is detected concerning the penetration of the CJ inside the mixing layer.

The §4 deals with the effects of the CJ nozzle geometry in terms of penetration, structures of the manipulated mixing layer and longitudinal vorticity.

4. Influence of the CJ nozzle geometry

For a fixed CJ stagnation pressure ($P_{CJ}=2,5\text{bar}$), we tested three kinds of CJ nozzle. The characteristics are shown in the table 1. We try here to separate the effects of the shape of the CJ nozzle (rectangular or circular), and the effects of the length scale (equivalent diameter). Note that the CJ type *rect2* and *circ* have the same equivalent diameter, and that the main difference between the CJ type *rect1* and *rect2* is the length of the small side of the nozzle.

4.1. CJ penetration

The CJ penetration information is obtained by the same technique as in §3.1.2. The figure 14 represent the average pictures obtained for each CJ nozzle. The global behaviour does not differ from one CJ type to the other: the CJ average trajectory does not seem to be affected by the shape or length scale of the nozzle. This may be due to the very sharp curvature of the CJ trajectory as it reaches the shear layer.

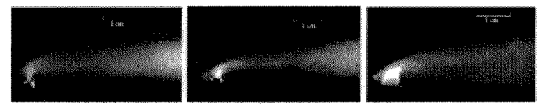


figure 14
Average side view for the CJ penetration
(from left to right: CJ type rect1, rect2 and circ)

The instantaneous pictures shown in figure 15 rise much interesting results. Although the rectangular CJ generate both the same kinds of structures, the behaviour is completely different for the circular CJ. Indeed, the CJ type *circ* never completely penetrates the shear layer. This may be caused by the fact that the longitudinal length scale of CJ type *circ* (e.g. the diameter) is far bigger than the rectangular ones, regarding the theoretical length of the Kelvin-Helmoltz structures. Taking $L_{KH}=15\text{mm}$ for the longitudinal structures spacing in front of the CJ nozzle exit, the longitudinal length scales of the CJ nozzles are:

$$\begin{cases} D_{circ} = L_{KH} / 3 \\ l_{rect1} = L_{KH} / 15 \\ l_{rect2} = L_{KH} / 7 \end{cases}$$

As a result, the transversal aspect of the structures of the CJ is not produced by the same mechanism.

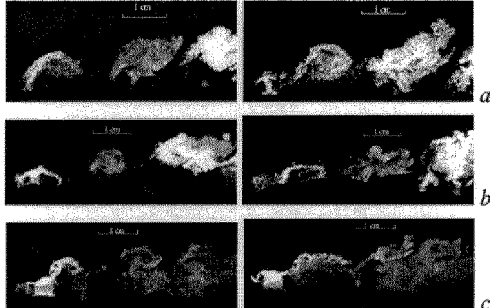


figure 15

Instantaneous side views for the three CJ nozzle types
(a:rect1 – b:rect2 – c:circ)

4.2. Longitudinal vorticity

The effects of the CJ geometry are firstly observed very near the CJ exit. The figure 16 shows a fundamental difference between the rectangular and the circular CJ nozzles. The first structures look like those observed in a curved pipe (Dean's vortices). They seem to match the size of the CJ thickness or diameter.



figure 16

Cross-sectional instantaneous views of the CJ
at $X/D=0.14$ (from left to right: rect1, rect2 and circ)

However, looking far downstream (see figure 17), we can see that all these structures rearrange themselves to a pair of counter rotating vortices.



figure 17

Cross-sectional instantaneous views of the CJ
at $X/D=0.6$ (from left to right: rect1, rect2 and circ)

Finally, the results obtained with the side and cross-sectional instantaneous pictures involve an important role of the CJ nozzle geometry on the structures generated in the very first stage of the interaction between the CJ and the free shear layer. The penetration behaviour is also strongly affected by the longitudinal length scale of the CJ nozzle. The next paragraph deals with the influence of the CJ geometry on the structures of the manipulated mixing layer.

4.3. Transversal aspect of the manipulated mixing layer

The figure 18 represents the average pictures obtained for the three CJ nozzles. The seeding is realised with ethanol droplets introduced in the boundary layer inside the main supersonic jet. The effects of the flow rate between the CJ and the main jet are obtained comparing the type *rect1* and *rect2*. It appears that a bigger CJ flow rate results in a more important mixing enhancement. The effects of the CJ nozzle shape is observed between CJ type *rect2* and *circ*, which have the same theoretical flow rate. No fundamental effect of the CJ nozzle shape issues from the average side views of the manipulated mixing layer.

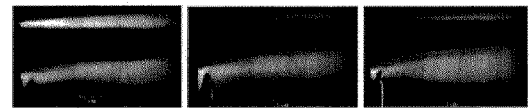


figure 18

Average side views of the manipulated mixing layer
(from left to right: CJ type rect1, rect2 and circ)

The figure 19 represents instantaneous side views of the manipulated mixing layer. Both CJ type *rect1* and *rect2* produce well-organised roll-ups in the mixing layer of the main jet. The distance separating these structures is not changed between CJ type *rect1* and *rect2*. However, as the height of the roll-ups is more important for case *rect2*, the Strouhal number is different between CJ type *rect1* and *rect2*.

The picture of figure 19 relative to CJ type *circ* reveals a very complex transversal arrangement of the structures of the mixing layer. Here again, the CJ nozzle geometry is a very important parameter of the size and the kind of the structures of the manipulated mixing layer.

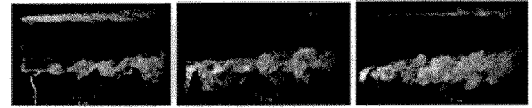


figure 19

Instantaneous side views of the manipulated mixing layer
(from left to right: CJ type rect1, rect2 and circ)

5. Conclusion

The pneumatic device seems to be a good mixing enhancement technique for supersonic jets. The spreading rate of the manipulated case is shown to be approximately 20% bigger than the natural spreading rate. An intermittent behaviour is detected for the CJ penetration in the mixing layer. The mechanism responsible of this behaviour is not well known. Two hypotheses can be done, involving the pressure fluctuations in the mixing layer, or an instability of the interaction between a transverse jet and a free shear layer. May be we could benefit by this intermittence to generate some kind of self pulsed CJ, although keeping a constant CJ stagnation pressure. One can imagine that a so called 'pseudo pulsed' CJ could produce an excitation of the natural Kelvin-Helmoltz modes of the mixing layer.

The study concerning the effects of the CJ nozzle geometry (size and shape) can be considered as a start point for future numerical developments. Since the visualisations presented in this paper put forward the very important part of the CJ geometry in the mechanisms of interaction with the mixing layer, a numerical simulation aiming at the optimisation of the CJ nozzle geometry must take into account the intermittent phenomena occurring in the near field of interaction between the main jet and the CJ.

The future developments of our investigations will concentrate on the intermittent behaviour detected for the penetration of the CJ into the free shear layer. We plan to determine the origins of this behaviour, mostly thanks to simple calculations. We also intend to evaluate the characteristics of the manipulated mixing layer: three-dimensional velocity field near injection, convective velocity of large eddies, and the structure organisation in the far field of the interaction.

References

- ¹ L.P. BERNAL & A. ROSHKO
"Streamwise vortex structure in a plane mixing layer"
J. Fluid Mech. (1986), vol. 170, pp 499-525
- ² J.K. FOSS & K.B.M.Q ZAMAN
"Large and small-scale vortical motions in a shear layer perturbed by tabs"
J. Fluid Mech. (1999), vol. 170, pp 499-525
- ³ L.J.S. BRADBURY & A.H. KHADEM
"The distortion of a jet by tabs"
J. Fluid Mech. (1975), vol. 70, part 4, pp. 801-813
- ⁴ K.B.M.Q ZAMAN, M.F. REEDER & M. SAMIMY
"Supersonic jet mixing enhancement by 'delta-tabs'"
AIAA paper 92-3548, July 1992
- ⁵ K.B.M.Q ZAMAN
"Axis switching and spreading of an asymmetric jet: the role of coherent structure dynamics"
J. Fluid Mech. (1996), col. 316, pp. 1-27
- ⁶ M.R. DAVIS
"Variable control of jet decay"
AIAA Journal (1982), vol. 20, n°5, pp 606-609
- ⁷ E. COLLIN, S. BARRE, J.P. BONNET
"Supersonic mixing enhancement by radial fluid injection"
Euromech Colloquium 403, Poitiers 2-4 nov. 1999